Ionospheric Scintillation Effects on Single and Dual Frequency GPS Positioning

S. Datta-Barua, P. H. Doherty, S. H. Delay, *Boston College*
T. Dehel, *FAA Technical Center, National Satellite Test Bed*
J. A. Klobuchar, *Innovative Solutions International, Inc.*

BIOGRAPHY

Seebany Datta-Barua is a research engineer studying low latitude ionospheric phenomena at the Boston College Institute for Scientific Research (ISR). She is also a Ph.D. candidate in the Aeronautics and Astronautics Department at Stanford University.

Patricia Doherty is a Senior Research Scientist with the Boston College ISR. Her prime research activities include studies of ionospheric effects on GPS signals and worldwide systems and in analytical and theoretical models of the earth's ionosphere.

Susan Delay is a Senior Research Analyst with the Boston College ISR. Her work includes data and numerical analysis, programming and graphics development.

Thomas Dehel is lead engineer on the National Satellite Test-Bed (NSTB), a prototype and test tool for the FAA's Wide Area Augmentation System (WAAS). He currently supports WAAS testing and related international and ionosphere test efforts.

John A. Klobuchar is a Chief Scientist for Atmospheric Research at Innovative Solutions International supporting the FAA in their development of the GPS Wide Area Augmentation System. He is also a Fellow of the IEEE.

ABSTRACT

The low latitude ionosphere poses a challenge to both GPS users and Satellite-Based Augmentation System (SBAS) providers. Single and dual frequency GPS receivers used in low-latitude regions can suffer from rapid amplitude and phase fluctuations known as scintillation. Scintillation occurs when the GPS or SBAS satellite signal travels through small-scale irregularities in electron density in the ionosphere, typically in the evening and nighttime in equatorial regions. Frequent scintillation and high rates of change in Total Electron Content (TEC) can cause loss of lock to dual frequency and even single frequency receivers. At these times, GPS users in low latitudes can experience decreased levels of accuracy and confidence in stand-alone positioning.

We present observations of scintillation and its effects on stand-alone positioning at a station in Rio de Janeiro, Brazil, during a two-week span in February of 2002, a post solar maximum year. A GPS Silicon Valley Ionospheric Scintillation Monitor (ISM) is colocated with a dual frequency MiLLennium™ receiver. The ISM provides measurements of amplitude scintillation at L1 once per minute via the S4 index of normalized standard deviation of signal intensity. Multipath can inflate S4, falsely indicating ionospheric scintillation activity, and is removed with the use of a multipath/scintillation discriminating technique.

Positioning is performed post-process by iteratively solving a linearized model of the range equations. For single frequency measurements, the ionosphere is estimated using the GPS broadcast ionospheric model. Dual frequency positioning has the advantage of exploiting direct measurements of TEC. We use carrier phase leveled measurements of TEC, when available, to estimate position accuracy available to a dual frequency user experiencing scintillation. For these TEC measurements the satellite and receiver inter-frequency biases have been estimated.

We present nighttime observations of TEC in Brazil and the relationship between high rates of TEC and amplitude scintillation. The effects of scintillation on both a single frequency receiver and dual frequency receiver's available constellation for positioning are shown. In addition, a dual frequency user's L2 availability is shown, as this impacts one of the main advantages of a dual frequency receiver: the ability to directly measure and remove the error due to the ionosphere. We aim to illustrate what kinds of effects the single frequency user and the dual frequency user can expect to experience, and what kind of result this can have on the accuracy and confidence in their position solutions.

INTRODUCTION

The ionosphere is a region of the atmosphere at an altitude of several hundred kilometers whose defining feature is the presence of free electrons stripped from atoms by solar ultraviolet radiation. As a dispersive medium that lies on the signal path between the orbiting GPS and Satellite-Based Augmentation System (SBAS) satellites and the users, the ionosphere refracts the broadcast RF wave by an amount proportional to the total electron content (TEC) along its path and as a function of the signal frequency. This error term is on the order of meters and affects GPS users worldwide.

Observed ionospheric behavior varies over the earth and can be generalized into auroral, mid-latitude, and equatorial areas. The geographic bands 10-15° north or south of the magnetic equator are referred to as the equatorial anomaly region, due to the occurrence of the Appleton anomaly. This anomaly is a daily evening-time peak in TEC that follows the local midday peak. The anomaly peak is both spatially and temporally highly variable and may reach higher magnitude than the midday peak. Small spatial irregularities in the ionosphere typically develop during and after the Appleton anomaly.

These small-scale irregularities in electron density can diffract the signal, leading to rapid fluctuations in signal intensity, known as amplitude scintillation [Skone 2000]. Amplitude scintillation can be severe enough that the received GPS signal intensity drops below a receiver's lock threshold, forcing the receiver to reacquire the signal [Doherty 2000]. Amplitude scintillation is measured by the S_4 index, which is essentially a normalized standard deviation in the signal intensity over 60 seconds.

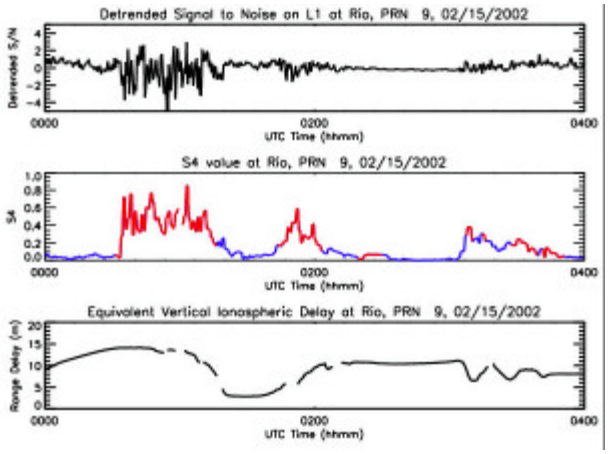

Figure 1: Ionospheric amplitude scintillation as captured by S/N, S4, and TEC measurements.

Figure 1 illustrates the characteristics of amplitude scintillation described above. The uppermost plot of detrended signal-to-noise ratio over time demonstrates that the receiver experiences a great deal of scintillation on this line of sight around 01:00 UT, and to a lesser extent at 02:00 and again after 03:00. The corresponding S_4 values, shown in the middle plot with the periods of scintillation highlighted in red, confirm these findings. The measurements of TEC are in the bottom plot, where distinctive ionospheric structure that coincides with periods of scintillation may be seen. The data shown in this plot are from the data set analyzed further in this paper, whose content and processing are described in subsequent sections.

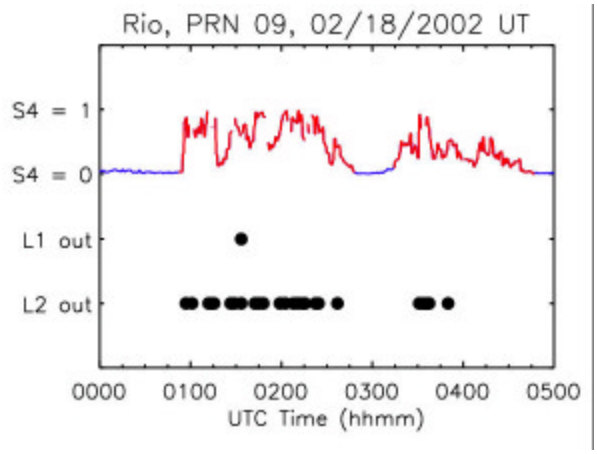

Figure 2: Effect of amplitude scintillation on availability of L1 and L2 data.

The effect of ionospheric amplitude scintillation on a GPS receiver is illustrated in Figure 2. The S_4 value at L1 along one line of sight is plotted across the top, with periods of scintillation highlighted in red (see description of S_4 data processing below). Epochs for which L1 measurements are unavailable, henceforth referred to as "dropouts" or "outages", are marked with black circles, as are L2 data outages. These dropouts are important because the loss or gain of a satellite's measurements effectively changes the available constellation of a user who wishes to perform stand-alone positioning. There is a correlation between periods of scintillation measured at L1 and the occurrence of dropouts on L2. This figure makes clear that scintillation can even be severe enough to cause data outages on the civilian L1 frequency. At its worst, scintillation can cause the very receiver designed to track it and provide the S_4 measurements to lose lock.

Another form of scintillation, known as phase scintillation, occurs from rapid phase variations in the signal after traveling through these same small-scale ionospheric irregularities. Phase scintillation may lead to cycle slips and loss of lock for receivers as they track the signal. Phase scintillation is quantified by $\sigma_{\Delta\varphi}$, the standard deviation of the detrended phase over an interval of up to 60 seconds. Phase scintillation is not addressed in this paper.

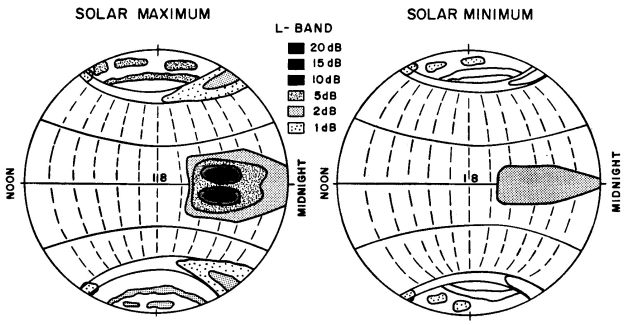

Figure 3: Fading depths at L-band worldwide for solar maximum and solar minimum.

Scintillation activity is both geographically and temporally dependent. The 11-year solar cycle, local season of the year, and geomagnetic location all play a role in degree of activity [Basu 1988]. Figure 3 shows the worldwide occurrence of worst-case fading at L-band frequencies during the peak of the solar cycle (left), and during solar minimum (right). The figure of the earth is oriented with the sunward-side on the left, and the nighttime side on the right. The strongest signal fading occurs for a few hours after sunset in the equatorial anomaly regions north and south of the magnetic equator and is more severe during heightened solar activity.

DATA AND IONOSPHERIC MEASUREMENT PROCESSING

The data analyzed and discussed in this paper come from two colocated stationary receivers in the equatorial anomaly region during a post-solar-maximum year. One source is NovAtel's dual frequency MiLLennium™ receiver, which tracks L1 and L2 (semi-codelessly) to provide pseudorange and carrier phase measurements at 30-second intervals. This receiver is part of the Brazilian Test-Bed (BTB) being developed by the FAA in South America.

The other receiver is the Ionospheric Scintillation Monitor (ISM) manufactured by GPS Silicon Valley (GSV). This receiver provides measurements of amplitude and phase scintillation at L1, in the forms of S_4 and $\sigma_{\Delta\varphi}$, updated at one-minute intervals. The ISM has wide-bandwidth tracking loops to maintain lock longer during the high rates of scintillation, and samples at a rate of 50 Hz to calculate the scintillation statistics S_4 and $\sigma_{\Delta\varphi}$ [Van Dierendonck 2001]. The wide bandwidth provides a considerable improvement in monitoring, but the ISM is still somewhat susceptible to extremely severe scintillation. In these cases it is forced to reacquire and accumulate data for four minutes before resuming output.

The receivers were placed in Rio de Janeiro, Brazil, which is located at 15° south magnetic latitude. These receivers recorded data from 15 – 28 February 2002, less than two years after the 2000 peak of the solar cycle. In the Americas, "scintillation season" takes place from September to March [Sobral 2002], so February is a reasonable time to expect to experience and measure scintillation.

TEC measurements are derived from the dual frequency data of the MiLLennium receiver. The carrier phase measurement of total electron content, expressed in meters at L1, is I_ϕ:

$$I_f^k = \frac{L1^k - L2^k}{g - 1}$$

Equation 1

$$I_r^k = \frac{P2^k - P1^k}{g - 1}$$

Equation 2

$$g = \left(\frac{f_1}{f_2} \right)^2$$

Equation 3

In these equations, $P1^k$ and $P2^k$ are the receiver pseudorange measurements, in meters, to the k^{th} satellite at the L1 and L2 frequencies, respectively; $L1^k$ and $L2^k$ are the carrier phase measurements to the k^{th} satellite, in meters; and f_1 and f_2 are the frequencies of the L1 and L2 bands, in Hz. The ionosphere is dispersive, and higher frequencies (i.e. L1 and L2 carrier signals) are advanced with respect to lower frequencies (i.e. chipping rates of code P1 and P2), so the signs for I_ρ and I_ϕ are opposite.

The code measurement of the ionospheric delay I_ρ is noisy but accurate. The carrier phase measurement I_ϕ is precise but ambiguous and subject to cycle slips. For these reasons, a cycle slip detector is used to identify likely cycle slips. The detrended third-order difference of the linear combination L1-L2 is iteratively tested for points beyond the larger of $|\pm 4\sigma|$ or $|\pm 1|$ (where $|*|$ indicates absolute value of the quantity enclosed) because cycle slips manifest themselves as extremely high rates of change in phase. Triple-differencing 30-second data requires continuous segments at least 2 minutes long; slips in anything shorter will remain undetected. Once the continuous segments of I_ϕ longer than 2 minutes are identified, they are piecewise leveled to the code measurement of the TEC, I_ρ. The broadcast satellite interfrequency bias known as T_{GD} is removed. The measurements may remain as slant delay for removal from the pseudorange measurements or be converted to equivalent vertical delay through use of a thin-shell

mapping function M that assumes a shell height of 350 km:

$$M(el^k) = \frac{1}{\cos(Sin^{-1}(\frac{R_e \cos(el^k)}{R_e + h_{iono}}))}$$

Equation 4

The mapping function M used is a thin shell model that is a function of the elevation of the k^{th} satellite. In the calculation of the obliquity factor M, R_e is the mean radius of the earth and h_{iono} is the assumed height of the ionospheric shell, in this case, 350 km. An estimate of the receiver L1/L2 interfrequency bias is made by exploiting the fact that unbiased TEC measurements have very consistent early morning equivalent vertical values across different lines of sight. We make use of this spatial uniformity by choosing the receiver interfrequency bias that minimizes the variance of the vertical TEC measurements each morning between UT 08:00 and 10:00, or 05:00-08:00 local time (LT).

Amplitude scintillation measurements S_4 were obtained at one-minute intervals from the ISM. These output measurements S_4 are given by:

$$S_4 = \sqrt{S_{4T}^2 - S_{4N}^2}$$

$$S_{4T} = \sqrt{\frac{\langle SI^2 \rangle - \langle SI \rangle^2}{\langle SI \rangle^2}}$$

Equation 5

S_{4T} is "total S_4" measuring fluctuations due to any cause and S_{4N} is a measure of amplitude fluctuations due to ambient noise described in more detail by Van Dierendonck [2001]. SI is signal intensity, measured at a frequency of 50 Hz, and <> indicates expected value of the quantity enclosed over a full minute. Since the variance of the signal intensity SI is normalized by the square of the average value of SI, and then the component of S_4 due to noise S_{4N} is removed, the resulting S_4 is a dimensionless number with a theoretical upper limit of 1.

Not only scintillation but also multipath interference can produce fluctuations in signal intensity. The periods when scintillation dominates the S4 value are distinguished through the use of a scintillation/multipath discriminator. This test makes use of the fact that the variance of the code-carrier divergence over 60 seconds is higher for multipath than for ionospheric phenomena. Conker et al. [2002] summarize a definition of multipath as occurring when the ratio of σ_{ccd} to S_4 is greater than 5. With the additional step of requiring that at least one quarter of the epochs in the previous 5 and subsequent 5 minutes must return a decision of "scintillation" for any given epoch to be considered a "scintillation" epoch itself, we are able to obtain more consistent results. This additional step is taken because the discriminator test has trouble distinguishing low elevation satellites whose signals are suffering multipath from ionospheric scintillation, so that at some epochs it mistakenly returns a decision of "scintillation" when there is no small-scale ionospheric disturbance visible in a plot of TEC. In plots of S_4 such as Figure 2, the periods when scintillation is determined to dominate the S_4 measurement are shown in red, and epochs when multipath is the main contributor to S_4 are shown in blue.

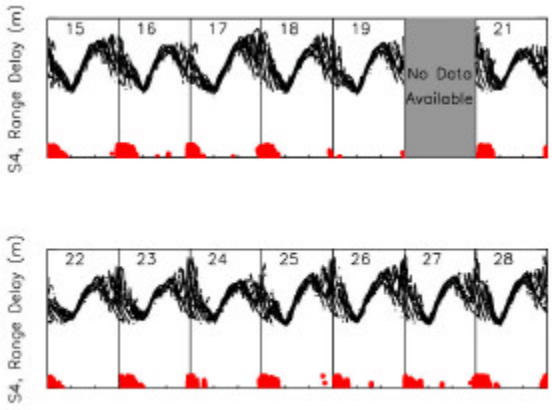

Figure 4: Summary of equivalent vertical TEC and S_4 measurements during scintillation from UT 15-28 February 2002.

Figure 4 shows equivalent vertical TEC measurements, derived as described above from the MiLLennium receiver, along every line of sight over the entire two-week period of the data set, which spans 15-28 February 2002. Below that curve, in red and not to scale, are the S4 measurements from the ISM, after filtering out all multipath-dominated measurements.

A number of general conclusions that we will use in looking at effects of scintillation on positioning can be drawn from this plot. First, in this region of the world at the equatorial anomaly during the stage of the solar cycle following peak activity, during the local scintillation season, we see that ionospheric scintillation happens almost nightly, generally from 00:00-06:00 UT (21:00-03:00 LT). The notable exception to this is 19 February, which is free of scintillation from 00:00-06:00 UT, and provides a quiet night for comparison of positioning.

A typical day of equivalent vertical TEC from this two-week data set is shown in greater detail in Figure 5. The period during which scintillation occurs, 00:00-06:00 UT, is characterized by wide variations in TEC from line-of-

sight to line-of-sight. Small-scale structure is also visible as more rapidly alternating periods of low TEC and high TEC. The period of scintillation follows the second daily equatorial anomaly peak. It occurs in the early evening after the midday peak, and is highly variable along each line of sight as well; notice that the anomaly peak is higher in magnitude than the midday peak, and happens at different times (from 19:00-24:00) on different lines of sight.

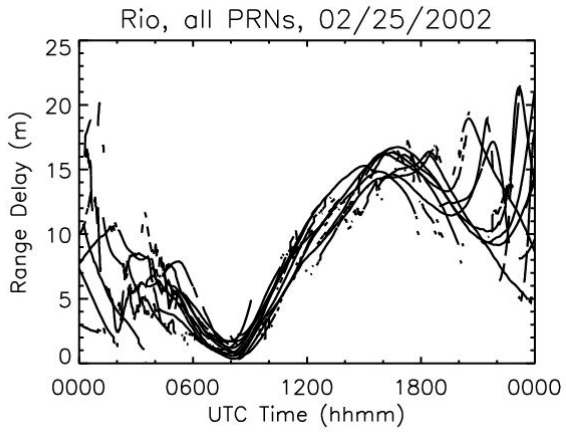

Figure 5: Equivalent vertical TEC on all lines of sight on a typical day with scintillation.

OCCURRENCE OF DATA OUTAGES

Amplitude scintillation can lead to data dropouts, as was seen in Figure 2. This is of concern to the GPS user because his constellation for positioning is affected by the gain or loss of satellites that apparently flicker in and out of visibility when scintillation or fading causes temporary loss of lock. The existence of a scintillation-free night in our data set, 19 February 2002, allows for the direct comparison of the total number of outages on that night between 00:00-06:00 UT versus all of the other nights.

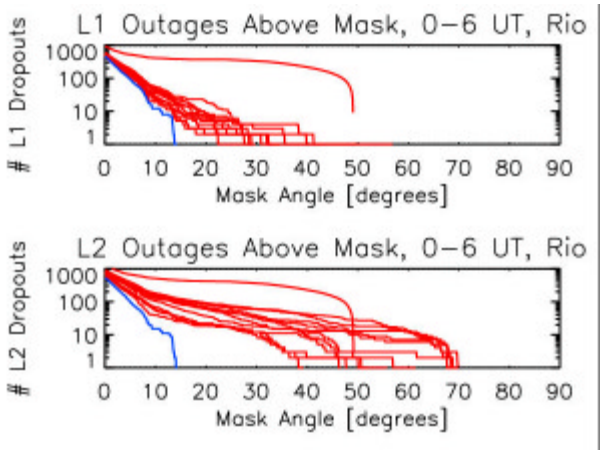

Figure 6: Number of data outages at L1 (top) and L2 as a function of mask angle.

The upper plot of Figure 6 shows the total number of outages (epochs during which the satellite was within view and healthy, but the receiver provided no information from it) at L1 from 00:00-06:00 UT as a function of mask angle, with one curve per night. The mask angle is the threshold elevation angle below which no data is considered.

The night on which there was no scintillation, 19 February, is drawn in blue. Notice that in spite of being scintillation-free, there are a significant number of data outages on satellites all the way up to an elevation el = 15°. For these low elevation satellites (el < 15°) on this quiet night, multipath was the likely culprit in causing data dropouts. However, on nights when there was scintillation *in addition to* this basic amount of multipath, there were outages on satellites at elevations up to 30° or even 40°. The curve that extends farthest to the right is inflated due to a single line of sight on 15 February for which the satellite was broadcast as healthy but was not tracked by the receiver for a few continuous hours while it was in the sky.

The lower plot in Figure 6 demonstrates the effect of scintillation on the number of outages at L2. On the quiet night, the receiver is still susceptible to outages up to 15° elevation. On the nights with observed scintillation, it is clear that high elevation satellites are even more likely to have L2 data drop out than L1, with outages existing on satellites almost as high as 70°.

The key features of this plot show that as baseline behavior in this data set we may expect outages up to 15° that may be due solely to multipath. Beyond that, scintillation is the dominating factor in dropouts.

Table 1 lists percentages of dropout frequency at L1. A user who is estimating position with a receiver comparable to the MiLLennium and is subject to scintillation may be interested to know how often she may expect to have dropouts on 1, 2, or 3 satellites simultaneously. For comparison we offer the same statistics calculated over the quiet night 19 February from 00:00-06:00 UT, as we do over all other nights from 00:00-06:00 UT combined.

Table 1

# svs	Without scint. (19 Feb)		With scint. (all others)	
out	5-15°	15-90°	5-15°	15-90°
1	11.7%	0%	14.7%	4.69%

#svs out	Without scintillation (19 February)	With scintillation (all others)
2	0.556%	2.50%
3	0%	0.289%

The GPS user estimating position on a scintillation-free night may lose exactly one low elevation (i.e. el < 15°) satellite just over 11% of the time. With scintillation exacerbating the multipath, the incidence of single low elevation satellite loss increases to over 14% of the time. On February 19th, there were no observed incidences of a single high elevation satellite being lost. Compare this to the other nights, when one high elevation satellite was out of view almost 5% of the time.

The lower half of Table 1 shows similar trends for the loss of 2 or 3 satellites simultaneously. On the quiet night, there were only a few epochs during which two satellites dropped out at the same time (corresponding to 0.556% of the time). With scintillation, a user may expect to lose 2 satellites at the same time 2.5% of the time, and some of them may be higher than 15°. A similar pattern follows for loss of 3 satellites.

The loss of L1 frequency data prevents the single- and also the dual- frequency user from including the satellite(s) in their constellation, and so is of concern to both. Similar outage percentages are calculated on L2, and are shown later, since they are applicable specifically to the dual-frequency user.

STAND-ALONE POSITIONING

The MiLLennium receiver dual frequency data are post-processed to estimate user position. The linearized model of the position equations can be found in many texts, for example, Misra [2001] or Strang [1997]. The technique involves iterating a weighted least squares solution on a linearized model of the position equations. Only satellites higher than 5° elevation are used for positioning. Prior to estimating user position, corrections must be applied to the vector of measured pseudoranges P1 at each epoch to arrive at a corrected pseudorange ρ in meters:

$$r = P1 + B \cdot c - I - T + (dt_S - b) \cdot c$$

Equation 6

These corrections include the list of broadcast satellite clock errors at the time of transmission B, converted to meters using the speed of light c; the ionospheric slant delay I for each satellite signal ray path, to be discussed in detail later for the single and dual frequency user; the tropospheric slant delays T for which we have used the dry component of a simple empirical model only [Misra 2001]; and the Sagnac correction dt_S, which accounts for the fact that the user is in a rotating reference frame - the earth - while using a clock [Parkinson 1996]. The user clock error b is one of the resulting estimates of the solution, and can be applied subsequent to the first iteration.

Beginning with an initial estimate of user location and clock bias x_0 that differs from the true position by some amount dx, the unit vectors between the position of each satellite at its time of transmission and the user position are arranged in the well-known geometry matrix G. The weighted least squares error solution for dx is then:

$$dx = (G^T W^{-1} G)^{-1} G^T W^{-1} r$$

Equation 7

The weighting matrix W will be specified for the single frequency and dual frequency users below. The error dx is added to the old estimate of position, and the process is repeated until the resulting errors are less than 10^{-4} m.

SINGLE FREQUENCY POSITIONING

The single frequency (SF) user solving for position must apply an ionospheric model correction $I = I_{model}$ in Equation 6 above. The model broadcast by the GPS satellites for SF users is described in detail in the Interface Control Document 200C. We apply as weighting matrix W in Equation 7 the one given by:

$$W^{-1}{}_{ij} = \begin{cases} (M(el^i)M(el^j))^{-1}, & i = j \\ 0, & i \neq j \end{cases}$$

Equation 8

Here, $M(el^i)$ is the obliquity factor for the i^{th} satellite whose expression is given in Equation 4.

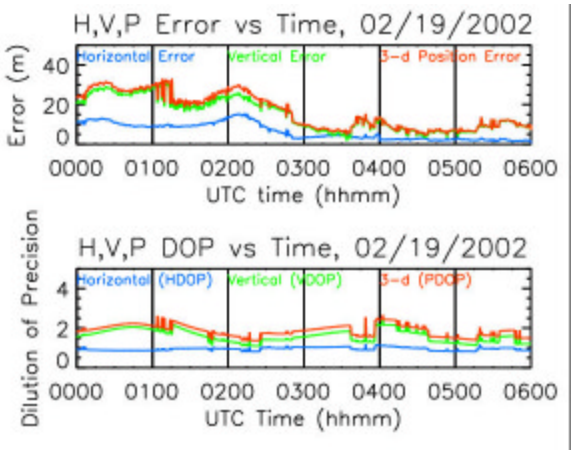

Figure 7: Position error vs time (top) and DOP vs time for single frequency user without scintillation.

The upper half of Figure 7 plots the single frequency user's position error in meters on the scintillation-free night, February 19th, from 00:00-06:00 UT. The

horizontal error is drawn in blue, the vertical error in green, and the 3-dimensional position error in red.

The lower plot of Figure 7 illustrates the corresponding dilution of precision (DOP) values. Dilution of precision is a unitless scalar derived from the geometry matrix G that characterizes the goodness of the constellation geometry. Lower DOP indicates better geometry for more precise positioning. The horizontal dilution of precision (HDOP) is shown in blue, vertical DOP (VDOP) in green, and 3-d position dilution of precision (PDOP) in red.

On this quiet night, the user's position error is as much as 30 m, and gradually decreases to about 10 m. The broadcast ionospheric model that the L1-only user must use does not account for the second daily anomaly peak in the equatorial regions. The error in estimation of the ionosphere at this time of night contributes to high magnitude position errors. Notice that after 01:00 UT the user position estimate and the DOP fluctuate rather than varying smoothly. An abrupt change in PDOP occurs when the constellation of satellites used in the position equations changes due to the rising or setting of a satellite. In this case, a low elevation ($5° < el < 15°$) satellite was setting, and as we have seen above, even on the scintillation-free night, low elevation satellites are susceptible to dropouts. The alternating loss and gain of this setting satellite cause the fluctuations in DOP and position error.

Since scintillation increases the likelihood of data outages, we expect to see more frequent fluctuations similar to this. In fact, Figure 8 shows exactly this. As an example of positioning on a typical night with scintillation, we have plotted similar position error and DOP plots for a scintillating night.

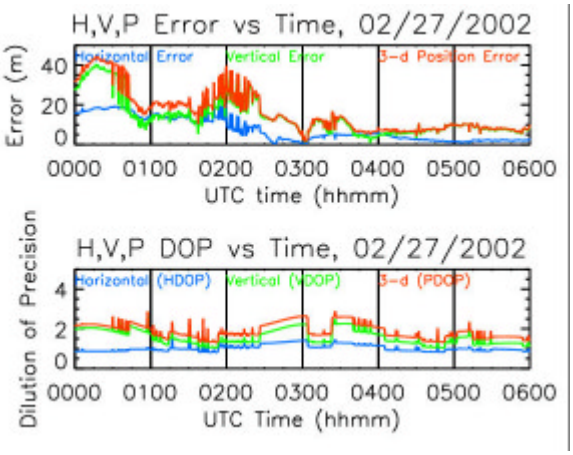

Figure 8: Position error vs time (top) and DOP vs time for single frequency user during scintillation.

On these nights the absolute position error may reach as high as 50 m. Notice that fluctuations in 3-d position and PDOP are much more frequent as satellites "flicker" in and out of view of the receiver. Higher rates of change in position error occur during scintillation. The fluctuations in position estimate can be on the order of 10 m. The loss or gain of low elevation satellites generally produce the most dramatic changes in position estimate, possibly because the SF model error estimate, which assumes a thin-shell ionosphere, diverges from the actual behavior of the ionosphere in the equatorial anomaly region.

The high rates of change in position estimate and DOP seen on this night are typical of all the nights on which scintillation occurred. The data depicted in Figure 9 for 15-28 February 2002 from top (red) to bottom (lower black curve) are: S4 due to scintillation (multipath epochs are not pictured), rate of change in 3-d position error, and rate of change in PDOP.

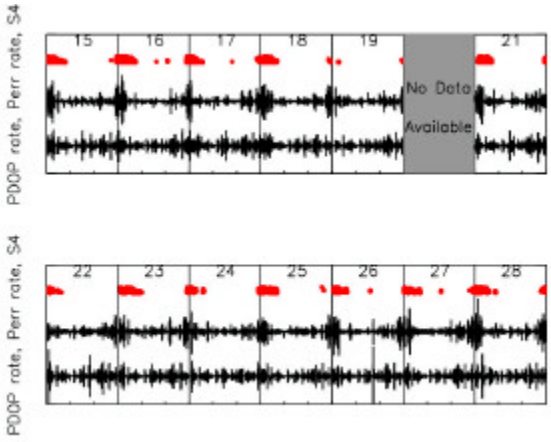

Figure 9: S_4 due to ionospheric scintillation, rate of change of 3-d position error, rate of change of PDOP over time span (UT) of data set.

The high magnitude rates of change in position estimate are visible on a nearly nightly basis around 0-6 UT. The exception to this is 19 February. On the 19th the standard deviation of the rate of change of 3-d position error of all estimates made between 00:00 and 06:00 UT was 1.7. Over the remaining nights (all of which showed scintillation activity), the position error rate of change was higher so that the standard deviation $\sigma = 2.9$. It is also clear from the plot that this bound on the rate of change during scintillation periods (0-6 UT) is significantly higher than at any other time of day. The rate of change of PDOP shows a less dramatic, but still significant, difference in spread on the scintillating nights compared to February 19th: compare $\sigma=0.121$ on the quiet night to $\sigma=0.189$ on the other nights. The nighttime fluctuations in DOP during scintillation happen with

higher frequency so that the variance from 00:00-06:00 UT is higher on all other nights than it is on the 19th.

We have seen an increase in fluctuations in the available constellation of the L1-only user due to amplitude-scintillation-induced data outages. The single frequency GPS stand-alone user relies on a thin-shell model of the ionosphere that, at equatorial latitudes, may differ from the actual ionosphere by 10s of meters, particularly during and after the second daily anomaly peak. As the ionospheric model correction for a satellite is added and removed from the position equations due to its fading in and out of view, the ionospheric error can translate into 3-dimensional position error as much as 50 m, and rapid fluctuations on the order of 10 m/epoch.

DUAL FREQUENCY POSITIONING

The dual frequency user has the capability to improve on the accuracy and precision of the single frequency GPS user through the use of the L2 frequency data for direct measurement of the ionospheric delay $I = I_{meas}$. For our analysis we use $I_{meas} = I_{\phi}$, which is calculated as described in Equations 2-3. For use in Equation 6, I_{ϕ} is not converted to equivalent vertical, but kept as a slant measurement. Measurement of the ionospheric group delay depends on the availability of L2. During scintillation, data transmitted on the L2 signal is more likely to be dropped, just as with L1. Below in Table 2 is a list of L2 outage percentages on the quiet night (19 February 2002) compared with all the other nights of the data set.

Since the L2 frequency does not contain a signal freely available to the civil community, commercially available receivers that employ codeless or (as with the MiLLennium) semi-codeless tracking to track L2 are more susceptible to loss of lock on L2 than L1. As a result, the overall percentages on both the quiet night and the active scintillation nights are higher than the corresponding values for L1. On the scintillation-free night 19 February, low elevation satellites (between 5° and 15°) were dropped 12.4% of the time. During scintillation this increased by more than 40% to a 17.5% chance of losing one low-elevation satellite. Whereas on the quiet night, L2 was never lost on any satellite above 15°, during scintillation hours from 0-6 UT, there was a 7.41% chance of losing exactly one high elevation satellite.

The lower table summarizes the percent of time that multiple satellite outages were observed simultaneously. On the 19th of February, 2 satellites dropped out simultaneously only rarely, and 3 never did. During scintillation 2 satellite outages happened at the same epoch more than 6% of the time, and 3 happened more than 1% of the time. In all, a dual-frequency user equipped with a receiver comparable to the one used here, the MiLLennium, might expect to spend almost one-third of his time without dual frequency data for some satellite or another in the constellation.

Table 2

# svs	Without scint. (19 Feb)		With scint. (all others)	
out	5-15°	15-90°	5-15°	15-90°
1	12.4%	0%	17.5%	7.41%

#svs out	Without scintillation (19 February)	With scintillation (all others)
2	0.694%	6.73%
3	0%	1.34%

A dual frequency user has a number of methods available for dealing with the inability to measure the ionospheric delay. Two options that we consider here are: 1) limiting the constellation available for positioning to only those satellites for which both L1 and L2 frequency measurements exist; 2) substituting the SF user's ionospheric error model for the satellites that have L1 only available, and de-weighting these terms in the position solution equations, since they are not likely to be as correct as the ionospheric measurement. We consider these two scenarios one at a time here.

DUAL FREQUENCY USER TYPE 1

Dual frequency (DF) users who limit their constellations to the satellites from which they are receiving both frequencies ("Type 1" users) solve the position Equations 6 and 7 with the use of an ionospheric correction *I* given by the code-leveled carrier phase measurement of ionospheric delay I_{ϕ} in Equation 2. In this scenario, the same elevation-dependent weighting matrix as the SF user's, given by Equation 8, is applied.

The DF Type 1 users enjoy significant improvement in accuracy, as is visible in Figure 10, which plots their position error over time on a scintillation-free night. Compared to the SF user, whose positioning for this same night is shown in Figure 7, the Type 1 user has 3-dimensional position errors under 20 m during the entire period from 00:00-06:00 UT. There is minimal fluctuation in this estimate even while the constellation changes. The constellation available to the Type 1 user is different from the SF user's, as can be seen by comparing the lower plots of DOP in Figures 7 and 10. The Type 1 user's constellation changes more often on the quiet night than the L1-only user's does, but this does not translate into large changes in position error because the Type 1 user measures the ionospheric delay error directly, whereas the SF user estimates it with a model that can differ from the true ionosphere in this part of the world at this time of night by 10s of meters slant.

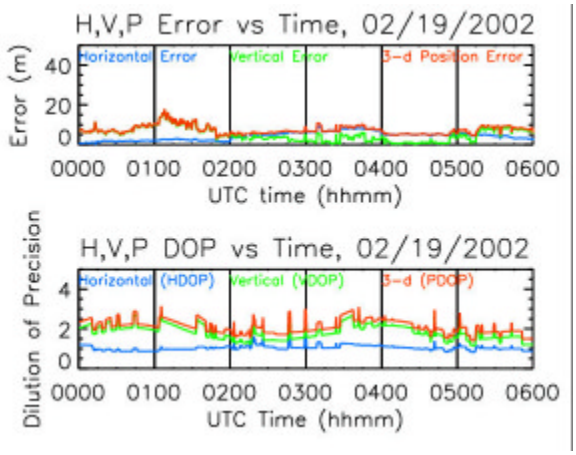

Figure 10: Position error vs time (top) and DOP vs time for dual frequency (Type 1) user without scintillation.

The DF Type 1 user who is now subjected to scintillation runs into different issues from the SF user. This is shown in the plots of horizontal, vertical, and 3-dimension position error and dilution of precision (DOP) in Figure 11.

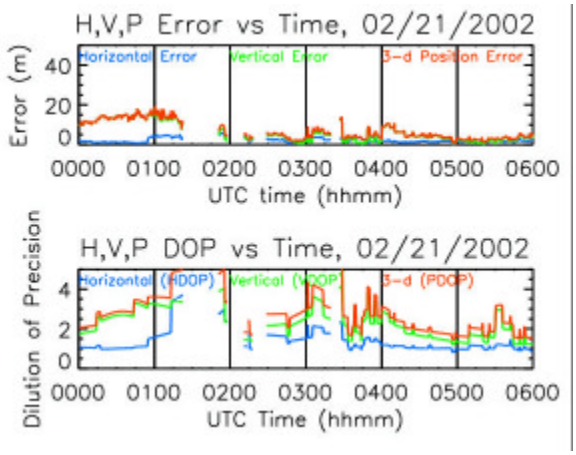

Figure 11: Position error vs time (top) and DOP vs time for dual frequency (Type 1) user during scintillation on 21 Feb 2002.

When a Type 1 user limits himself to satellites from which he has received both L1 and L2 frequency data, dropouts and cycle slips will hurt his ability to calculate a position *at all*. He may be often limited to too few satellites (less than 4) to solve for position. In general, due to cycle slips and data dropouts, we observed that there were fewer than 4 satellites available for positioning 8.46% of the time during scintillation. This percentage will vary with implementation of cycle slip detection, correction, and receiver capability.

In addition there are situations where there may be at least 4 satellites in view, but due to the physical location of the actively scintillating ionosphere at that time, the remaining constellation provides such poor geometry that the position estimate cannot be reliably trusted. In our positioning software, we have required a geometrical dilution of precision (three spatial dimensions plus time) of GDOP < 10. From an error-propagation standpoint, DOPs are multiplicative factors for errors being propagated through from the range domain to the position domain. Hence lower DOPs are better, and beyond a certain threshold the receiver position cannot be reliably calculated. With the caveat that such a number is dependent on the cycle slip detection and patching algorithms as well as the receiver's tracking capabilities, we observed a GDOP > 10 about 17% of the time from 0-6 UT on the scintillating nights.

For direct comparison with the SF user, compare Figure 11 with Figure 12 below. The SF user with a receiver comparable to the MiLLennium will be able to estimate position during scintillation, but it may differ from the true position by 10s of meters. The dual frequency Type 1 user has traded availability of a position solution for accuracy of under 20 m.

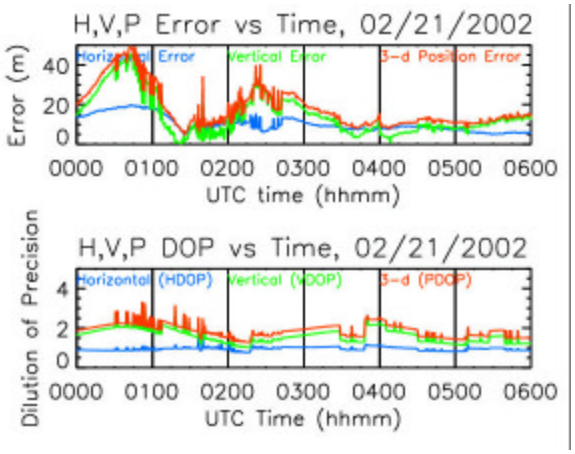

Figure 12: Position error vs time (top) and DOP vs time for single frequency user on 21 Feb 2002.

DUAL FREQUENCY USER TYPE 2

Another method by which the dual frequency user may account for the loss of L2 data is by compensating for lost ionospheric measurements by using the SF user's model of the ionosphere instead. We will refer to this user's scenario as that of the Type 2 dual frequency user. The Type 2 DF user may thereby hope to combine the position availability of the SF user with a degree of accuracy approaching that of the DF (Type 1) user.

In combining ionospheric measurement terms I_{meas} with ionospheric model terms I_{model} in the vector I in Equations

6 and 7, the Type 2 user accounts for the fact that the model diverges from the true ionospheric delay, and places less emphasis on these terms when solving for the weighted least squares solution. The Type 2 user's choice of ionospheric correction term *I* is given by:

$$I = \begin{cases} I_{meas} = I_f = \dfrac{L1 - L2}{g - 1}, & if\ \exists\ P2^k\ and\ L2^k \\ I_{\mathrm{mod}\,el}, & otherwise \end{cases}$$

Equation 9

The expression for γ is given in Equation 3. The weighting matrix W we implement is:

$$W^{-1}{}_{ij} = \begin{cases} (M(el^i)M(el^j))^{-1}, & i = j\ and\ \ P2^k\ and\ L2^k\ \ exist \\ (M(el^i)M(el^j))^{-2}, & i = j\ and\ \ P2^k\ or\ L2^k\ \ not\ exist \\ 0, & i \neq j \end{cases}$$

$$M(el^k) = \frac{1}{\cos(Sin^{-1}(\dfrac{R_e \cos(el^k)}{R_e + h_{iono}}))}$$

Equation 10

The resultant Type 2 position estimation on a night with scintillation can be seen in Figure 13 and compared to the SF position error and DOP plot (Figure 12) or the dual frequency Type 1 user's position error and DOP plot (Figure 11).

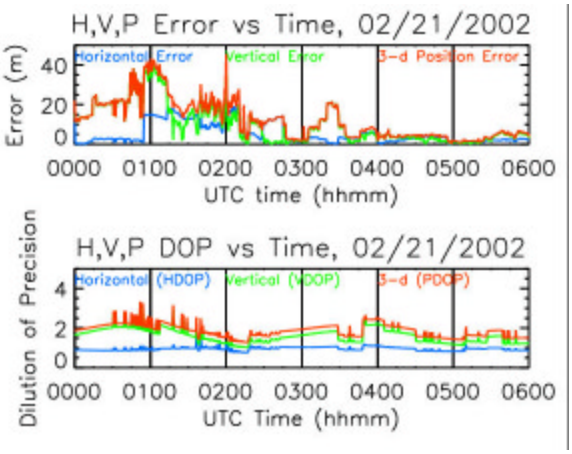

Figure 13: Position error vs time (top) and DOP vs time for dual frequency (Type 2) user during scintillation on 21 Feb 2002.

Because the Type 2 user keeps in her constellation all satellites for which any data is available (i.e. L1 frequency data), the constellation which determines the DOP plots for the SF user and this Type 2 user are identical.

The 3-dimensional position error reaches 40 m at times, almost as high as the SF user error, and at times decreases as low as the Type 1 user error. During the period when the Type 1 user was entirely unable to make a position estimate between 01:30 and 02:30 UT, the DF Type 2 user has enough satellites and good enough geometry (GDOP < 10) to estimate position. The error at this time is comparable to that of the SF user in magnitude and fluctuation. The Type 2 DF user has ceded some positioning accuracy in order to increase availability to that of the SF user.

CONCLUSIONS

Amplitude scintillation due to the early nighttime ionosphere impacts both single and dual frequency GPS users in the equatorial anomaly region of the world. Scintillation increases the frequency of data outages on both L1 and L2, both for low elevation satellites whose signals are subject to multipath and for high elevation satellites that are usually clear in the receiver's view. This in turn changes the user's available constellation for positioning.

The single frequency user can expect high rates of change in position estimate due to loss of L1 data, combined with large absolute errors due to the secondary peak in TEC of the ionospheric phenomenon known as the "anomaly". The dual frequency user has the advantage of being able to measure the ionosphere directly, but is susceptible to more frequent L2 dropouts and cycle slips since civilian receivers track the L2 frequency codelessly or semi-codelessly. Type 1 dual frequency users, who limit their constellation to all satellites for which ionospheric estimates are available, have high accuracy but worse geometry. At times they may even lack position estimates altogether during scintillation. Type 2 dual frequency users, who substitute the single frequency ionospheric model correction broadcast by the GPS satellites into the position equations when the measurement is unavailable, and de-weight the model-corrected terms, have availability and DOP identical to L1-only users. Their absolute errors can be as low as the Type 1 users', but may also reach as high as the single frequency GPS users'.

Further tuning of the weighting matrix W of the Type 2 dual frequency user who solves for position by weighted least squares estimation, may improve the overall accuracy of this method when used during scintillation. Another technique that may be considered when an ionospheric measurement is unavailable to the dual frequency user is the reuse of the most recent ionospheric measurement, with filtering over time. One important consideration in this case would be the fact that amplitude scintillation often accompanies small-scale irregularities

in the ionosphere. The total electron content might be rapidly changing just at the moment when the dual-frequency measurement was lost, which would put a limit on the duration that an old measurement might be considered valid or safe to reuse.

ACKNOWLEDGEMENTS

The authors would like to thank the FAA WAAS program for funding this research. Thanks also to Dr. Todd Walter for providing helpful feedback and comments.

REFERENCES

Basu, S., MacKenzie, E., and Basu, Su., "Ionospheric Constraints on VHF/UHF Communications Links During Solar Maximum and Minimum Periods," *Radio Science*, vol. 23, no. 3, 1988.

Conker, R.S. and El-Arini, B., "Preliminary Analysis of the Effects of Ionospheric Scintillation on the MTSAT Satellite-Based Augmentation System (MSAS)," Ionospheric Effects Symposium, Alexandria, VA, 5-7 May 2002, p. 167-178.

Doherty, P., "Ionospheric Scintillation Effects in Equatorial and Auroral Regions," ION GPS 2000, Salt Lake City, Utah, p. 662-671.

Interface Control Document 200C, *NAVSTAR GPS Space Segment / Navigation User Interface*, Arinc Research Corporation: El Segundo, California, 10 October 1993.

Misra, P., and Enge, P., *Global Positioning System: Signals, Measurement, Performance*, Ganga-Jamuna Press: Lincoln, Massachusetts, 2001.

B. W. Parkinson, J. J. Spilker, P. Axelrad, and P. Enge eds., *Global Positioning System: Theory and Applications*, vol. 1-2, American Institute of Aeronautics andAstronautics, Washington, D.C., 1996.

Skone, S., "Impact of Ionospheric Scintillation on SBAS Performance," ION GPS 2000, Salt Lake City, Utah, p. 284-293.

Sobral, J.H.A., et al., "Ionospheric Plasma Bubble Climatology Over Brazil Based on 22 Years(1977-1998) of 630 nm Airglow Observations," *Journal of Atmospheric and Solar-Terrestrial Physics*, vol. 64 (2002), p. 1517-1524.

Strang, G. and K. Borre, *Linear Algebra, Geodesy, and GPS*, Wellesley-Cambridge Press: Wellesley, Massachusetts, 1997.

Van Dierendonck, A.J., and Hua Q., "Measuring Ionospheric Scintillation Effects from GPS Signals," ION 59th Annual Meeting, Albuquerque, New Mexico, 11-13 June 2001, p. 391-396.

"Detection and Repair of Cycle Slips," *Principles and Practice of GPS Surveying*, retrieved 23 Apr 2002 from University of New South Wales, Satellite Navigation and Positioning web site updated 18 Jan 2000: http://www.gmat.unsw.edu.au/snap/gps/gps.survey/chap7/735.htm.